Magnetic Resonance in Medicine 47:392–397 (2002)

Relationships Between Diffusion Tensor and *q*-Space MRI

Peter J. Basser*

Fundamental relationships between diffusion tensor (DT) and 3D *q*-space MRI are derived which establish conditions when these two complementary MR methods are equivalent. It is shown that the displacement distribution measured by *q*-space MRI in both the large displacement (i.e., large r) and the long-wavelength (i.e., small *q*) limits is the same 3D Gaussian displacement distribution assumed in DT-MRI. In these limiting cases, *q*-space MR yields a dispersion tensor that is identical to the effective DT, D, measured in DT-MRI. An experiment is then proposed to measure D using *q*-space methods. These findings establish that the effective DT, measured in DT-MRI, characterizes molecule motions on a coarse length-scale. Finally, the feasibility of and requirements for performing 3D *q*-space MRI on a clinical scanner are considered. Magn Reson Med 47: 392–397, 2002. Published 2002 Wiley-Liss, Inc.†

Key words: *q*-space; NMR; diffusion tensor; MRI; DTI; DT-MRI; DSI

Concepts of *q*-space NMR are increasingly informing NMR and MRI studies of tissue structure-function relationships, particularly in brain white matter. Several groups have employed *q*-space NMR concepts to measure features of the translational displacement distribution of water molecules within white matter, primarily to investigate its microstructure and organization and their possible alterations in disease (1–8). In principle, this method could demonstrate the existence of restriction (i.e., impermeable barriers); characterize water mobility in distinct anatomical compartments within axons, axon bundles, and fascicles (e.g., Ref. 2); and even help resolve differences in the orientations of distinct white matter tracts (7).

Displacement distributions have also been measured in tissues such as anisotropic white matter, using diffusion tensor MRI (DT-MRI) (9). However, there is no existing framework by which to compare and contrast *q*-space and DT-MRI experimental findings. In fact, there is a gap in our understanding of the fundamental theoretical relationships that exist between these two distinct MR methods. The development of such a conceptual schema could substantially advance many areas of research in tissue biology and materials science.

Specifically, in this work we address several key questions: Are DT and *q*-space MRI methods complementary and consistent? How are the displacement distributions measured by *q*-space and DT-MRI methods related? Can *q*-space MRI methods also be used to measure an effective DT? If so, how is this quantity related to the effective DT measured by DT-MRI? More generally, how are the *q*-space and DT-MRI formalisms related, and in what cases are their results directly comparable? Does the analysis of the *q*-space MRI experiment provide fresh insights into the physical meaning of the effective DT or provide limits on its range of experimental applicability? Is *q*-space MRI clinically feasible? In the process of addressing these questions, we describe mathematical methods that can be used to relate *q*-space and DT-MRI experiments.

BACKGROUND

Building on Stejskal and Tanner's (10,11) pulsed-field gradient (PFG) spin-echo experiments, and their novel interpretation of them, several studies (12–14) proposed *q*-space NMR to investigate the microscopic motion of spins in complex materials. This NMR method provides a direct measurement of the displacement distribution of an ensemble of spins without requiring an explicit model of the translational diffusion process. Also, *q*-space NMR allows one to assess separately the effects of changes in diffusion time, orientation, and length-scale probed, on the displacement distribution.

In establishing a correspondence between *q*-space and DT-MRI experiments, we start by considering the behavior of spins in the *q*-space experiment in the coarse-scale limit. The canonical *q*-space NMR experiment is performed using a PFG sequence (see Fig. 1 for an example) for which two key conditions must be satisfied: First, the width of the diffusion gradient pulse, δ, is considered to be infinitesimally short. The gradient pulse waveform, $\mathbf{G}(t)$, can then be represented as a delta-function with area $\mathbf{G}\,\delta$, so that

$$\mathbf{q} = \frac{\gamma}{2\pi}\int_0^t \mathbf{G}(t)dt = \frac{1}{2\pi}\gamma\mathbf{G}\delta. \qquad [1]$$

Thus, $\mathbf{q}$ is no longer explicitly a function of time, t, but only a function of the duration of the phase-encoding period, δ. Second, molecular displacements taking place during the application of these short diffusion gradient pulses are assumed to be negligibly small compared to the displacements that occur during the diffusion time, Δ, between these pulses, i.e., $\delta \ll \Delta$.

When both these assumptions are satisfied, the conditional translational displacement distribution of tagged spins, $P(\mathrm{r}_2, \Delta \,|\, \mathrm{r}_1, 0)$, and the normalized echo attenuation, $E(\mathbf{q}, \Delta)$, are related by (10):

$$E(\mathbf{q}, \Delta) = \int_{-\infty}^{\infty}\int_{-\infty}^{\infty} P(\mathbf{r}_2, \Delta|\mathbf{r}_1, 0)P(\mathbf{r}_1)e^{i\mathbf{q}\cdot(\mathbf{r}_2-\mathbf{r}_1)}d^3\mathbf{r}_2 d^3\mathbf{r}_1 \qquad [2]$$

Section on Tissue Biophysics and Biomimetics, NICHD, National Institutes of Health, Bethesda, Maryland.

Grant sponsor: Israel–U.S. Binational Science Foundation; Grant number: 97-00346.

*Correspondence to: Peter J. Basser, Ph.D., National Institutes of Health, Bldg. 13, Rm. 3W16, 13 South Drive, Bethesda, MD 20892-5772. E-mail: pjbasser@helix.nih.gov

Received 15 February 2001; revised 14 September 2001; accepted 27 September 2001.

DOI 10.1002/mrm.10052

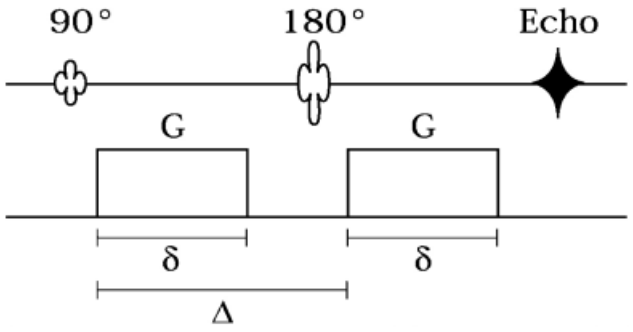

FIG. 1. The Stejskal-Tanner PFG sequence used in a *q*-space NMR experiment. Included in the spin-echo sequence are two gradient pulses with magnitude G, pulse duration δ, and diffusion time Δ. The conditions that must be satisfied in *q*-space NMR are that δ is infinitesimally short, and $\delta \ll \Delta$.

where $E(\mathbf{q})$ is the complex NMR signal attenuation measured at $\mathbf{q}$. $P(\mathbf{r}_2, \Delta \mid \mathbf{r}_1, 0)$ is the probability that a spin-labeled molecule starting at position $\mathbf{r}_1$ at time 0 ends up at position $\mathbf{r}_2$ at time Δ; $P(\mathbf{r}_1)$ is the initial distribution of spins. If one further assumes local homogeneity, the displacement distribution then depends only upon the net displacement, $\mathbf{r} = \mathbf{r}_2 - \mathbf{r}_1$, not on the initial or final positions of the molecules per se, so that $P(\mathbf{r}_2, \Delta \mid \mathbf{r}_1, 0) = P(\mathbf{r}, \Delta \mid \mathbf{0}, 0)$. Furthermore, if one assumes that the spin density is uniform in the excited volume, i.e., $P(\mathbf{r}_1)$ is constant, then Eq. [2] above reduces to:

$$E(\mathbf{q}, \Delta) = \int_{-\infty}^{\infty} P(\mathbf{r}, \Delta|\mathbf{0}, 0) e^{i\mathbf{q}\cdot\mathbf{r}} d^3\mathbf{r}. \quad [3]$$

The integral above is a 3D Fourier transform of $P(\mathbf{r}, \Delta \mid \mathbf{0}, 0)$ with respect to the displacement vector, $\mathbf{r}$. The inverse Fourier transform (F^{-1}) of $E(\mathbf{q}, \Delta)$ in Eq. [3] yields $P(\mathbf{r}, \Delta \mid \mathbf{0}, 0)$:

$$P(\mathbf{r}, \Delta|\mathbf{0}, 0) = \int_{-\infty}^{\infty} E(\mathbf{q}, \Delta) e^{-i\mathbf{q}\cdot\mathbf{r}} d^3\mathbf{q} = F^{-1}(E(\mathbf{q}, \Delta)). \quad [4]$$

The mathematical framework and formalism required to perform 3D *q*-space MRI are well established and can be found in numerous articles and textbooks on *q*-space MRI methods, such as Ref. 13. The *q*-space formalism used in NMR spin-echo experiments is formally similar to earlier quasi-elastic incoherent neutron scattering experiments (e.g., see Ref. 39) in which one measures the intermediate scattering function. This equivalence was also pointed out by Callaghan (13). However, explicit relationships between *q*-space and DT-MRI methods have not been proposed. That is the subject of the analysis below.

THEORY

Large Displacement or Large-r Limit

To establish an explicit relationship between *q*-space and DT-MRI formalisms, we examine the asymptotic behavior of the displacement distribution in Eq. [4] in the limit of large $\mathbf{r}$. This is the case in which the diffusing species can probe the material over a length-scale larger than the size of inclusions and restrictive domains. Specifically, we use a variant of an asymptotic expansion method, Laplace's method[1] (e.g., Ref. 15) to study the behavior of $\lim_{r\to\infty} P(\mathbf{r},\Delta|\mathbf{0},0)$.

We first rewrite $E(\mathbf{q})$ using the following identity:

$$E(\mathbf{q}, \Delta) = e^{\ln(E(\mathbf{q},\Delta))} \quad [5]$$

so that Eq. [4] becomes:

$$P(\mathbf{r}, \Delta|\mathbf{0}, 0) = \int_{-\infty}^{\infty} e^{\ln(E(\mathbf{q},\Delta))} e^{-i\mathbf{q}\cdot\mathbf{r}} d^3\mathbf{q}. \quad [6]$$

Now, in the large-r limit, the function $e^{-i\mathbf{q}\cdot\mathbf{r}}$ that modulates $E(\mathbf{q})$ in Eq. [6] oscillates rapidly. Watson's lemma (15) guarantees that the integral can be adequately approximated by examining the behavior of the integrand only near its maximum at $\mathbf{q} = \mathbf{0}$. Thus, we expand the exponent, $\ln(E(\mathbf{q}))$, as a complex Taylor series about $\mathbf{q} = \mathbf{0}$. However, because $P(\mathbf{r}_2, \Delta \mid \mathbf{r}_1, 0)$ is a positive real function, the real part of $E(\mathbf{q})$ is an even function of $\mathbf{q}$, and the imaginary part of $E(\mathbf{q})$ is an odd function of $\mathbf{q}$. The real part of $E(\mathbf{q})$ can then be written as a Taylor series:

$$\ln(E(\mathbf{q})) \cong \ln(|E(\mathbf{0})|) + \frac{1}{2|E(\mathbf{0})|} \sum_{k=1}^{3}\sum_{j=1}^{3} q_k \, |E(\mathbf{q})|_{,kj}|_{\mathbf{q}=\mathbf{0}} \, q_j + O(q^4). \quad [7]$$

Above, q_k indicates the k^{th} component of $\mathbf{q}$, and "$,_{kj}$" indicates partial differentiation with respect to q_k and q_j. Since $|E(\mathbf{0})| = 1$, it follows that $\ln(|E(\mathbf{0})|) = 0$. Therefore, Eq. [7] simplifies to:

$$\ln(E(\mathbf{q})) \cong \frac{1}{2}\sum_{i=1}^{3}\sum_{j=1}^{3} q_i \, |E(\mathbf{q})|_{,ij}|_{\mathbf{q}=\mathbf{0}} \, q_j + O(q^4). \quad [8]$$

The leading real term in Eq. [8] is a quadratic form whose 3 × 3 Hessian matrix, $|E(\mathbf{q})|_{,ij}|_{\mathbf{q}=\mathbf{0}}$, is symmetric[2] and negative definite. By defining $\underline{\mathbf{H}}$ as follows:

$$\frac{1}{2}\sum_{i=1}^{3}\sum_{j=1}^{3} q_i \, |E(\mathbf{q})|_{,ij}|_{\mathbf{q}=\mathbf{0}} \, q_j = -\frac{1}{2}\mathbf{q}^T\underline{\mathbf{H}}\mathbf{q} \quad \text{where} \quad \mathbf{H}_{ij} = -|E(\mathbf{q})|_{,ij}|_{\mathbf{q}=\mathbf{0}} \quad [9]$$

we see that $\underline{\mathbf{H}}$ is both positive definite and symmetric. One way to interpret $\underline{\mathbf{H}}$ is that its three eigenvalues are the three principal curvatures that characterize the shape of $|E(\mathbf{q})|$ near $\mathbf{q} = \mathbf{0}$.

[1]This method is widely used in the theory of complex variables to obtain the asymptotic behavior of integrals.

[2]Technically, only the symmetric part of the matrix can make a non-zero contribution in the quadratic form.

Finally, to obtain the asymptotic form of the displacement distribution, we substitute Eqs. [8] and [9] into Eq. [6]:

$$\lim_{\mathbf{r}\to\infty} P(\mathbf{r}, \Delta|\mathbf{0}, 0) = \int_{-\infty}^{\infty} e^{-1/2\ \mathbf{q}^T\underline{\mathbf{H}}\mathbf{q}} e^{-i\mathbf{q}\cdot\mathbf{r}} d^3\mathbf{q}. \qquad [10]$$

Eq. [10] is the 3D Fourier transform of a 3D Gaussian probability density function of $\mathbf{q}$. The result is a 3D Gaussian probability density function of the random variable $\mathbf{r}$:

$$\lim_{\mathbf{r}\to\infty} P(\mathbf{r}, \Delta|\mathbf{0}, 0) \approx e^{-1/2\ \mathbf{r}^T\underline{\mathbf{H}}^{-1}\mathbf{r}}. \qquad [11]$$

Further examination of Eq. [11] leads to a second interpretation of $\underline{\mathbf{H}}$. It is the covariance matrix of a 3D Gaussian displacement distribution obtained by taking expected values of the mean-squared displacements along the x, y, and z directions:

$$\underline{\mathbf{H}} = \langle \mathbf{r}\mathbf{r}^T \rangle = \begin{pmatrix} \langle x^2 \rangle & \langle xy \rangle & \langle xz \rangle \\ \langle xy \rangle & \langle y^2 \rangle & \langle yz \rangle \\ \langle xz \rangle & \langle yz \rangle & \langle z^2 \rangle \end{pmatrix}. \qquad [12]$$

Moreover, the three eigenvalues of $\underline{\mathbf{H}}$ are the three principal mean-squared displacements along its three principal directions at a diffusion time Δ.

We can now make a formal connection between the displacement distributions measured using q-space NMR methods (in the large-r limit) and DT-NMR. Just as the one uses the Einstein equation to define an apparent diffusion coefficient (ADC) (13,16) as the mean-squared displacement divided by twice the diffusion time, we define the effective or apparent DT, $\underline{\mathbf{D}}$, as the mean-squared displacement tensor, $\underline{\mathbf{H}}$, defined in Eq. [12], divided by twice the diffusion time, or:

$$\underline{\mathbf{H}} = 2\underline{\mathbf{D}}\Delta \quad \text{thus} \quad \underline{\mathbf{H}}^{-1} = \frac{1}{2\Delta}\underline{\mathbf{D}}^{-1}. \qquad [13]$$

Equation [13] is simply a 3D generalization of the Einstein equation (17) appropriate for a homogenous anisotropic medium[3]. Substituting $\underline{\mathbf{D}}^{-1}$ for $\underline{\mathbf{H}}^{-1}$ using Eq. [13], and incorporating the proper normalization constants in the Gaussian distribution in Eq. [11] above, we obtain the final result:

$$\lim_{\mathbf{r}\to\infty} P(\mathbf{r}, \Delta|\mathbf{0}, 0) = \frac{1}{\sqrt{|\underline{\mathbf{D}}|(4\pi\Delta)^3}}\, e^{-\mathbf{r}^T\underline{\mathbf{D}}^{-1}\mathbf{r}/(4\Delta)}. \qquad [14]$$

The Gaussian displacement distribution, Eq. [14], is exactly the one we assume in DT-NMR (18) and DT-MRI (9). Because this derivation does *not* depend on the explicit details of the diffusion process, such as the number of distinct compartments, the conditions at their boundaries, the exchange between compartments, etc., this result is quite general.

We can now relate the echo attenuation and the effective DT in the q-space MRI experiment in the large-r regime. Substituting the Gaussian distribution in Eq. [14] into Eq. [3], we immediately obtain:

$$|E(\mathbf{q})| = e^{-4\pi^2\mathbf{q}^T\underline{\mathbf{D}}\mathbf{q}\Delta} \quad \text{or} \quad \ln(|E(\mathbf{q})|) = -4\pi^2\mathbf{q}^T\underline{\mathbf{D}}\mathbf{q}\Delta. \qquad [15]$$

We also recognize Eq. [15] as Stejskal's solution to the modified Torrey-Bloch equation for a PFG sequence in which $\Delta >> \delta$ (10).

The form of Eq. [15] above suggests how to measure $\underline{\mathbf{D}}$ using q-space methods so that q-space and DT-MRI experiments can be directly compared. The entire DT can be estimated statistically from Eq. [15] by acquiring at least seven diffusion-weighted images, at least six of which are obtained by applying gradients that are not coplanar and not collinear. Since each diffusion-weighted signal, $|E(\mathbf{q}_n)|$, represents a projection of the DT along a different gradient direction specified by $\mathbf{q}_n$, i.e., $\mathbf{q}_n^T\ \underline{\mathbf{D}}\ \mathbf{q}_n$, the measured effective DT is the one that yields the best fit of the $|E(\mathbf{q}_n)|$ data to Eq. [15] (in a least-squared sense). Thus, the optimal $\underline{\mathbf{D}}$ can be statistically estimated by minimizing χ^2:

$$\chi^2 = \sum_{n=1}^{N} \frac{1}{\sigma_n^2} (|E(\mathbf{q}_n)| - e^{-4\pi^2\mathbf{q}_n^T\underline{\mathbf{D}}\mathbf{q}_n\Delta})^2 \qquad [16]$$

for N ($\geq$7) diffusion-weighted signals by using Eq. [15] just as in DT-NMR (18) and DT-MRI (9). This proposed q-space NMR experiment to measure $\underline{\mathbf{D}}$ does not assume a priori that the material's intrinsic or principal coordinate system is given or known with respect to the laboratory frame of reference—for example, as it is in Refs. 13 and 19.

The equation used to measure $\underline{\mathbf{D}}$ in the DT-MRI experiment (18) is based on a solution to the modified Torrey-Bloch equation, also derived by Stejskal (10), in which the condition $\Delta >> \delta$ is relaxed. Nonetheless, the effective DT measured using q-space MRI methods in the large-r limit, using Eq. [16] above, is the same quantity as the apparent or effective DT one measures using DT-MRI. So, if performed correctly, q-space NMR in the small q limit should produce the same effective DT as DT-NMR.

Long-Wavelength or Small-q Limit

Another perspective on how q-space and DT-MRI methods are related can be attained by studying $|E(\mathbf{q})|$ in the long-wavelength limit, i.e., as $q \to 0$. In one dimension, it is useful to rewrite the signal attenuation in Eq. [3] as the expected value of the complex phase (20):

$$|E(q_z, \Delta)| = \mathrm{Re}(\langle e^{-2\pi i q_z Z} \rangle) \sim 1 - 2\pi^2 q_z^2 \langle Z^2 \rangle + O(q_z^4). \qquad [17]$$

The NMR signal attenuation caused by random displacements along the Z direction clearly show a quadratic dependence on q_z in the small-q limit (20,21). If one uses the

[3]The definitions of $\underline{\mathbf{H}}$ and $\underline{\mathbf{D}}$ are consistent with definitions of the mean-squared displacement and diffusion coefficient in the Einstein equation describing diffusion in an isotropic medium, i.e., $\mathrm{Trace}(\underline{\mathbf{H}}) = \mathrm{Trace}(\langle \mathbf{r}\ \mathbf{r}^T \rangle) = \langle \mathbf{r}^T\mathbf{r} \rangle = \langle \mathbf{r}\cdot\mathbf{r} \rangle = \langle r^2 \rangle = 2\mathrm{Trace}(D)\Delta = 6\langle D \rangle\Delta$.

Einstein equation, $\langle Z^2 \rangle = 2D\Delta$, to define an effective diffusivity, D, then one immediately obtains:

$$|E(q_z, \Delta)| \sim 1 - 4\pi^2 q_z^2 D\Delta + O(q_z^4). \quad [18]$$

Generalization of this result to three dimensions is straightforward:

$$|E(\mathbf{q}, \Delta)| = \mathrm{Re}(\langle e^{-2\pi i \mathbf{q}\mathbf{r}} \rangle) = 1 - 2\pi^2 \mathbf{q}^T \langle \mathbf{r}\,\mathbf{r}^T \rangle \mathbf{q} + O(q^4)$$
$$= 1 - 2\pi^2 \mathbf{q}^T \underline{\mathbf{H}} \mathbf{q} + O(q^4) \quad [19]$$

where we have used Eq. [12] above. Again, using the generalized Einstein equation given in Eq. [13] to relate the covariance of the displacement distribution and the effective DT, one immediately obtains:

$$|E(\mathbf{q}, \Delta)| = 1 - 4\pi^2 \mathbf{q}^T \underline{\mathbf{D}} \mathbf{q} \Delta + O(q^4). \quad [20]$$

Clearly, to second order in $\mathbf{q}$, one cannot distinguish the decay of $|E(\mathbf{q})|$ in Eq. [20] to that of Eq. [15], which is produced by assuming a 3D Gaussian displacement distribution for $\mathbf{r}$. This finding is also consistent with Stepisnik's analysis of Eq. [17] using the method of cumulants (22) in the Gaussian limit. Thus, in the small-q regime, we can treat the quadratic decay of $|E(\mathbf{q})|$ vs. q as arising from a Gaussian displacement distribution.

Finally, what remains is to establish a relationship between q-space MRI and DT-MRI. Since q-space NMR is compatible with k-space encoding (13), the incorporation of a PFG q-space diffusion sequence within an imaging sequence does not inherently change the relationship between the measured echo attenuation and the measured displacement distribution. The same holds between DT-NMR and DT-MRI. Generally, in diffusion imaging, if the imaging gradients are immediately refocused (23–27), or imaging and diffusion sequences are separated, then the effect of imaging gradients on diffusion attenuation can be decoupled. Thus, results of a properly performed q-space MRI experiment at large-r should be consistent with those of a DT-MRI experiment as well.

DISCUSSION

Are DT-NMR and DT-MRI measurements informative in the small displacement or short-wavelength limits? Probably not. While these methods certainly can be and have been applied in the large-q regime, the interpretation of the effective DT as a physically significant quantity is limited to the small-q or large-r regimes, where it describes the behavior of diffusing spins at the coarsest macroscopic length-scales. In tissues, large-r operationally corresponds to the regime in which the logarithm of the signal attenuation decreases linearly with the amount of diffusion weighting, as measured by Trace($\underline{\mathbf{b}}$), where $\underline{\mathbf{b}}$ is the b-matrix[4] (18). In the mammalian brain, this linear range is associated with values of Trace($\underline{\mathbf{b}}$) that lie between 0 and about 1000 (28) to 2000 s/mm^2 (29). If appropriate multicompartment models of diffusion are employed, perhaps the range of b-values can be extended to higher b-values.

Are q-space NMR and MRI clinically feasible, even in the large displacement or long-wavelength limits? Probably not using existing gradient technology. Unlike DT-MRI, which makes modest demands on gradient hardware and is currently performed on scanners equipped with whole-body gradient sets, q-space MRI requires short-duration diffusion gradient pulses with rapid rise times that even the most advanced whole-body (or head) gradient systems can not provide. Typical diffusion-weighted imaging (DWI) parameters used to acquire DT-MRIs are $\delta \sim 50$ ms, $\Delta \sim 60$ ms, and TE ~ 120 ms, with a maximum diffusion gradient strength of approximately 4 G/cm. Clearly, DWI acquired with these timing parameters fail to satisfy either requirement of q-space NMR, i.e., that the gradient pulse be "large and infinitely short" and that $\delta << \Delta$. For comparison, a typical q-space NMR acquisition could have parameters: $\delta \sim 1$ ms, $\Delta \sim 100$ ms, and TE $\sim$ 130 ms, with a maximum diffusion gradient strength of approximately 500–1000 G/cm (13).

Current U.S. Food and Drug Administration (USFDA) regulations (30), which are based upon patient health and safety concerns, pose another obstacle to performing q-space MRI clinically. The peak rate of change of the magnetic field (dB/dt_{max}) produced during a low-r q-space acquisition by a 100-cm whole-body gradient set is approximately 125,000 T/s (= 250 G/cm × (100/2) cm/0.01 ms). This dB/dt_{max} is orders of magnitude larger than the dB/dt thresholds associated with peripheral nerve stimulation (PNS) and pain (31–33). Recent FDA guidelines (i.e., $dB/dt_{max} \sim 20$ T/s for a gradient pulse with a rise-time of 1 ms; $dB/dt_{max} \sim 100$ T/s for a rise time of 0.1 ms; and $dB/dt_{max} \sim 1000$ T/s for a rise time of 0.01 ms) preclude such a high dB/dt in MRI acquisitions (30). Interestingly, even in a "large-r" q-space MRI experiment, dB/dt_{max} would be exceeded (i.e., dB/dt ~ 10 G/cm × 50 cm/0.01 ms = 5000 T/s).

Conditions for performing q-space MRI on the human brain are somewhat more favorable using a small head gradient set, but are by no means ideal. Based on reasonable head coil performance specifications, dB/dt is still close to PNS and pain thresholds (i.e., dB/dt ~ 10 G/cm × 10 cm/0.1 ms = 100 T/s).

Nonetheless, Tuch et al. (7) have reported using conventional DWIs acquired on a clinical scanner to measure a 3D displacement distribution of water molecules in vivo at high "q." While their method, diffusion spectrum imaging (DSI), uses the formalism of 3D q-space MRI, it does so without satisfying its essential requirements. First, in DSI, δ is not infinitesimally short (i.e., $\delta \approx 50$ ms) (7). In brain parenchyma, this pulse duration corresponds to a root mean square displacement of water molecules of about 10 μm, which is comparable to the dimensions of cells and significantly *larger* (not smaller) than other potentially restrictive compartments. Second, in DSI, $\delta \approx \Delta$ (7). Thus, virtually all of the diffusive motion takes place during the encoding period, δ, rather than during the diffusion time, Δ.

On a more fundamental level, in DSI q is no longer meaningfully interpreted as an inverse wavelength, and

[4]In DT-MRI, the b-matrix plays an analogous role to $|\mathbf{q}|^2\Delta$ in q-space MRI: it contains the factors premultiplying the elements of the DT in the formula relating the signal attenuation and the DT.

the diffusion time, Δ, is ill defined. The simple Fourier relationship (Eq. [4]) between the echo attenuation and a displacement distribution no longer applies. Even when one employs the "propagator" concept (34), it is not clear how to interpret the calculated "displacement distribution" or explain how it is related to the 3D displacement distribution one would obtain using existing and well established *q*-space MRI methods (13). Finally, according to the arguments given above, DSI should provide the same displacement distribution and effective DT as DT-MRI in the "large-r" and long-wavelength regimes. However, no such confirmatory study has been performed to date.

While the intermediate **q** and **r** ranges are extremely important biologically, there are significant obstacles to using conventional 3D *q*-space MRI to probe this regime using DWIs in which small-amplitude, long-duration diffusion gradient pulses are applied. While one could apply the formalism of Caprihan et al. (35) or Callaghan (36) in the "forward problem" (i.e., to predict the changes in $E(\mathbf{q})$ when the structure of the medium is known a priori), there is no comparable methodology to help us solve the "inverse problem" (i.e., to infer the underlying microstructure a posteriori from $E(\mathbf{q})$). Unfortunately, the latter is the problem we typically encounter in biological and clinical applications. The elegant "center of mass" formalism of Mitra and Halperin (37) clearly demonstrates that as the duration of the diffusion gradient pulse, δ, increases, the ability to deconvolve the details of the molecular displacements decreases, and that the artifactual sharpening of the measured displacement distribution increases as the constant gradient limit is approached (38).

CONCLUSIONS

The asymptotic behavior of the displacement distribution in *q*-space NMR is Gaussian in the large-r limit. In this regime, *q*-space MRI yields an effective DT, $\underline{\mathbf{D}}$, identical to that measured using DT-MRI methods. Our analysis results in two interesting interpretations of this quantity: First, $\underline{\mathbf{D}}$ is proportional to the Hessian matrix of $|E(\mathbf{q})|$ at $\mathbf{q} = \mathbf{0}$, which characterizes the curvature of $|E(\mathbf{q} = \mathbf{0})|$. Second, $\underline{\mathbf{D}}$ is proportional to the covariance matrix of the Gaussian displacement distribution that is obtained in the large-r limit. A series approximation is used to examine the signal attenuation, $|E(\mathbf{q})|$, in the long-wavelength or low-*q* regime. Again, in this limit, the decay of $|E(\mathbf{q})|$ with respect to q is also consistent with a Gaussian displacement distribution to order q^4. These findings suggest that the effective DT characterizes molecular motion on a coarse length-scale, and is most appropriately used in the large-r or low-*q* regimes. We also suggest a new scheme to measure $\underline{\mathbf{D}}$ using *q*-space MRI methods.

Our analysis demonstrates that DT and *q*-space MRI methods are entirely complementary and compatible methodologies, although they use different formalisms. DT-NMR and DT-MRI can be performed meaningfully using long-duration diffusion gradient waveforms that are closely separated in time, so they can be performed in a whole-body scanner. However, order-of-magnitude estimates suggest that the strong, short-duration gradient pulses required for *q*-space MRI preclude its use on clinical scanners equipped with whole-body gradient sets, *even in the large-r or long-wavelength regimes*. *q*-Space MRI does provide additional spatial, temporal, and orientational information about molecular displacements which is not provided by DT-MRI, and, at present, is particularly well suited to studying small animals, small tissue samples, and other biological specimens.

ACKNOWLEDGMENTS

Thanks go to Alan Barnett, who carefully examined the asymptotic analyses and made many useful suggestions to improve them. Sinisa Pajevic, Carlo Pierpaoli, Derek Jones, and Dick Shrager critically read various drafts of this work and made many constructive suggestions, as did Mark Horsfield. Larry Latour and Janez Stepisnik offered insights about *q*-space NMR. Liz Salak edited the manuscript. Thanks go to the Israel-US Binational Science Foundation for their continued support, and to Yoram Cohen, whose long-time interest in using *q*-space concepts in biological applications stimulated much of this work.

REFERENCES

1. Assaf Y, Cohen Y. Structural information in neuronal tissue as revealed by *q*-space diffusion NMR spectroscopy of metabolites in bovine optic nerve. NMR Biomed 1999;12;35–44.
2. Assaf Y, Mayk A, Cohen Y. Displacement imaging of spinal cord using *q*-space diffusion-weighted MRI. Magn Reson Med 2000;44;713–722.
3. Assaf Y, Cohen Y. Assignment of the water slow-diffusing component in the central nervous system using *q*-space diffusion MRS: implications for fiber tract imaging. Magn Reson Med 2000;43;191–199.
4. King MD, Houseman J, Roussel SA, van Bruggen N, Williams SR, Gadian DG. *q*-Space imaging of the brain. Magn Reson Med 1994;32; 707–713.
5. King MD, Houseman J, Gadian DG, Connelly A. *q*-Space imaging of the brain. In: Proceedings of the 3rd Annual Meeting of ISMRM, Nice, France, 1995. p 353.
6. King MD, Houseman J, Gadian DG, Connelly A. Localized *q*-space imaging of the mouse brain. Magn Reson Med 1997;38;930–937.
7. Tuch DS, Weiskoff RM, Belliveau JW, Wedeen VJ. High angular resolution diffusion imaging of the human brain. In: Proceedings of the 7th Annual Meeting of ISMRM, Philadelphia, 1999. p 321.
8. Wedeen VJ, Reese TG, Tuch DS, Weigel MR, Dou J-G, Weiskoff RM, Chessler D. Mapping fiber orientation spectra in cerebral white matter with Fourier-transform diffusion MRI. In: Proceedings of the 8th Annual Meeting of ISMRM, Denver, 2000. p 82.
9. Basser PJ, Mattiello J, Le Bihan D. MR diffusion tensor spectroscopy and imaging. Biophys J 1994;66;259–267.
10. Stejskal EO. Use of spin echoes in a pulsed magnetic-field gradient to study restricted diffusion and flow. J Chem Phys 1965;43;3597–3603.
11. Stejskal EO, Tanner JE. Spin diffusion measurements: spin echoes in the presence of time-dependent field gradient. J Chem Phys 1965;42; 288–292.
12. Cory DG, Garroway AN. Measurement of translational displacement probabilities by NMR: an indicator of compartmentation. Magn Reson Med 1990;14;435–444.
13. Callaghan PT. Principles of nuclear magnetic resonance microscopy. Oxford: Oxford University Press; 1991.
14. Callaghan PT, Eccles CD, Xia Y. NMR microscopy of dynamic displacements: k-space and q-space imaging. J Phys E: Sci Instrum 1988;21;820–822.
15. Carrier G, Crook M, Pearson CE. Functions of a complex variable: theory and technique. New York: McGraw-Hill; 1966.
16. Tanner JE. Self diffusion of water in frog muscle. Biophys J 1979;28: 107–116.
17. Einstein A. Investigations on the theory of the Brownian movement. New York: Dover Publications, Inc.; 1926.

18. Basser PJ, Mattiello J, Le Bihan D. Estimation of the effective self-diffusion tensor from the NMR spin echo. J Magn Reson B 1994;103: 247–254.
19. Callaghan PT, Jolley KW, Lelievre J. Diffusion of water in the endosperm tissue of wheat grains as studied by pulsed field gradient nuclear magnetic resonance. Biophys J 1979;28:133–141.
20. Callaghan PT, Codd SL, Seymour JD. Spatial coherence phenomena arising from translational spin motion in gradient spin echo experiments. Concepts Magn Reson 1999;11:181–202.
21. Callaghan PT, Stepisnik J. Generalized analysis of motion using magnetic field gradients. Adv Magn Reson 1996;19:325–388.
22. Stepisnik J. Validity limits of Gaussian approximation in cumulant expansion for diffusion attenuation of spin echo. Physica B 1999;270: 110–117.
23. Hsu EW, Mori S. Analytical expressions for the NMR apparent diffusion-coefficients in an anisotropic system and a simplified method for determining fiber orientation. Magn Reson Med 1995;32:194–200.
24. Le Bihan D. Molecular diffusion nuclear magnetic resonance imaging. Magn Reson Q 1991;7:1–30.
25. Mattiello J, Basser PJ, Le Bihan D. Analytical expression for the b matrix in NMR diffusion imaging and spectroscopy. J Magn Reson A 1994;108:131–141.
26. Mattiello J, Basser PJ, Le Bihan D. Analytical calculation of the b matrix in diffusion imaging. In: Bihan DL, editor. Diffusion and perfusion magnetic resonance imaging. New York: Raven Press; 1995. p 77–90.
27. Mattiello J, Basser PJ, Le Bihan D. The b matrix in diffusion tensor echo-planar imaging. Magn Reson Med 1997;37:292–300.
28. Pierpaoli C, Jezzard P, Basser PJ, Barnett A, Di Chiro G. Diffusion tensor MR imaging of the human brain. Radiology 1996;201:637–648.
29. DeLano MC, Cooper TG, Siebert JE, Potchen MJ, Kuppusamy K. High-b-value diffusion-weighted MR imaging of adult brain: image contrast and apparent diffusion coefficient map features. AJNR Am J Neuroradiol 2000;21:1830–1836.
30. Zaremba LA. Guidance for the submission of premarket notifications for magnetic resonance diagnostic devices. U.S. Department of Health and Human Services, Food and Drug Administration, Center for Devices and Radiological Health, 1998.
31. Bourland JD, Nyenhuis JA, Schaefer DJ. Physiologic effects of intense MRI gradient fields. Neuroimaging Clin North Am 1999;9:363–377.
32. Frese G, Hebrank FX, Renz W, Storch T. Physikalische Parameter bei der Anwendung der MRT. Radiologe 1998;38:750–758.
33. Ham CGL, Engels JML, van de Wiel GT, Machielsen A. Peripheral nerve stimulation during MRI: effects of high gradient amplitudes and switching rates. J Magn Reson Imaging 1997;5:933–937.
34. Kärger J, Heink W. The propagator representation of molecular-transport in microporous crystallites. J Magn Reson 1983;51:1–7.
35. Caprihan A, Wang LZ, Fukushima E. A multiple-narrow-pulse approximation for restricted diffusion in a time-varying field gradient. J Magn Reson A 1996;118:94–102.
36. Callaghan PT. A simple matrix formalism for spin echo analysis of restricted diffusion under generalized gradient waveforms. J Magn Reson 1997:129:74–84.
37. Mitra PP, Halperin BJ. Effects of finite gradient-pulse widths in pulsed field-gradient diffusion measurements. J Magn Reson 1995;113:94–101.
38. Sen PN, Andre A, Axelrod S. Spin echoes of nuclear magnetization diffusing in a constant magnetic field gradient and in a restricted geometry. J Chem Phys 1999;111:6548–6555.
39. Chen SH, Kotlarchyk M. Interaction of photons and neutrons with matter. Singapore: World Scientific; 1997.